

REMOTE RAMAN SPECTROSCOPY OF SALTS AND ORGANICS IN THE SUBSURFACE OF ICE – A POTENTIAL INSTRUMENT FOR EXPLORING EUROPA. S. K.Sharma¹, J. N. Porter¹, A. K. Misra¹, T. E. Acosta-Maeda¹, S. M. Angel², and C. P. McKay³, ¹Univ. of Hawaii, Honolulu, HI 96822, USA, e-mail: shiv@hawaii.edu, ²Dept. of Chem. & Biochem., Univ. of South Carolina, Columbia, SC 29208, USA, ³NASA Ames Research Center, Space Science Division, Moffett Field, CA 94035, USA.

Introduction: Europa's icy surface is thought to hide a global subsurface ocean more than twice that of Earth's Ocean [1, 2] with potential for microbial life [e.g., 3, 4]. Analysis of Near Infrared Mapping Spectrograph (NIMS) data from the *Galileo* spacecraft identified the presence of hydrous magnesium sulfate and sulfuric acid on Europa surface [e.g., 5, 6]. Linear mixture modeling of cryogenic laboratory spectra of hydrated compounds fitted to NIMS observations were used to predict abundances of hydrated compounds. According to these predictions Europa's dark, non-water-ice terrain contains 14% magnesium hexahydrate, 11% bloedite ($(\text{Na}_2\text{Mg}(\text{SO}_4)_2 \cdot 4\text{H}_2\text{O})$), 12% mirabilite ($\text{Na}_2\text{SO}_4 \cdot 10\text{H}_2\text{O}$), and 62% sulfuric acid hydrate [7]. Recently Dalton et al. [8] have compared sulfuric acid hydrate ($\text{H}_2\text{SO}_4 \cdot n\text{H}_2\text{O}$) abundance derived from NIMS observations with weathering patterns and intensities associated with charged particles from Jupiter's magnetosphere. From this study, these authors have concluded that the sulfuric acid hydrate production on Europa appears to be limited in some regions by a reduced availability of sulfur ions, and in others by insufficient levels of electron energy. Surface deposits in these regions of limited exogenic processing are likely to bear closest resemblance to oceanic composition [8].

One key to understanding the nature of Europa is to precisely determine whether the composition of the icy surface reflects the interior ocean chemistry. These and other questions regarding subsurface organics and biogenic materials largely remain unresolved with NIMS instrument. In the Science Definition Report on Europa [9] Raman spectroscopy has been identified as one of the techniques for a future Europa Lander [10].

Remote Raman spectroscopy has been demonstrated for detecting minerals, organic and biogenic materials at radial distances of ≥ 100 m distance [11, 12] as well as from a robotic platform [13]. In the present work, we have evaluated the performance of a remote Raman system at 120 m distance by measuring Raman spectra of various percentage of $\text{MgSO}_4 \cdot 7\text{H}_2\text{O}$ (epsomite) salt, and polyaromatic hydrocarbons (PAHs) naphthalene and anthracene, and dry ice (CO_2 -ice) inside crushed H_2O -ice, shaved H_2O -ice, and H_2O -ice to simulate Europa's surface environment. PAHs were selected due to their presence in the interstellar medium, in comets and meteorites, and are presumed

to have played a major role in the origin of life on the early Earth.

Experimental Methods: The portable pulsed remote Raman system in the coaxial monostatic system used in the present study is described in detail elsewhere [16]. In brief, the remote Raman system consists of an 8-inch (203.2 mm) diameter Meade telescope, a frequency-doubled mini Nd:YAG pulsed laser source (Quantel Laser, CFR model, 532 nm, 100 mJ/pulse, 15 Hz, pulse width 10 ns), 10x beam expander, and a Kaiser Optical Systems f/1.8 HoloSpec spectrometer equipped with a gated, thermoelectrically cooled intensified charge-coupled device (ICCD) detector (Princeton Instruments) and 50 μm slit. The laser beam from a 10x beam expander is made collinear with the telescope's optical axis by using two 45-degree mirrors. The telescope is directly coupled to the spectrometer through a camera lens (50 mm, f/1.8). A 532-nm holographic SuperNotch filter from Kaiser Optical Systems is placed at the back of the telescope to minimize the reflected and Rayleigh-scattered photons from the target.

Sample Preparation: H_2O -ice blocks of 25x15x5 cm^3 were prepared by freezing tap water in a deep (187 K) freezer. The shaved H_2O -ice samples were prepared from these blocks using a shave-ice machine. Crushed water-ice samples containing 10 wt% epsomite ($\text{MgSO}_4 \cdot 7\text{H}_2\text{O}$) and 1 wt% of naphthalene (C_{10}H_8) were also prepared. The samples of synthetic epsomite, naphthalene, and anthracene ($\text{C}_{14}\text{H}_{10}$) were in 25 mm diameter glass bottles and were buried under various thickness of the H_2O -ice and shaved H_2O -ice before making remote Raman measurements. Similarly dry ice (CO_2 -ice) samples contained inside plastic bag were also buried under various thickness of the H_2O -ice and shaved H_2O -ice for remote Raman measurements.

Results and Discussion: Figure 1 shows the Raman spectra of liquid water, H_2O -ice block, epsomite in crushed ice, and beyond a 5 cm layer of shaved H_2O -ice at 120 m distance. In the spectrum of liquid water, strong broad Raman bands at 3270 and ~ 3440 cm^{-1} are due to symmetric and antisymmetric stretching O-H vibrational modes of water molecules, respectively. The Raman spectrum of ice (Fig. 1) shows bands around the same spectral region as water, but it has a very strong and sharp band at 3140 cm^{-1} , making

it easily distinguishable from liquid water. The decrease in the frequency of symmetric O-H stretching

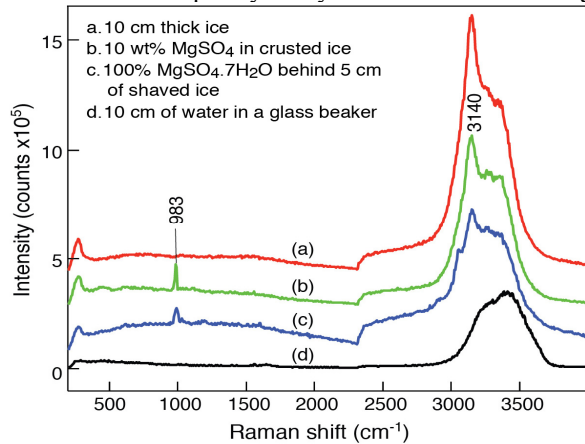


Figure 1. Raman spectra of liquid- and solid-H₂O-ice, and epsomite sample inside H₂O-ice at 120 m (laser 532 nm, 100 mJ/pulse, 15 Hz, slit width 50 μ m; integrated over 15 laser shots).

mode of water molecules in ice is due to formation of stronger hydrogen bond in ice. In the Raman spectrum of 10% MgSO₄ in crushed ice (Fig. 1) the hydrated sulfate is easily detected by the presence of SO₄ symmetric stretching ($\nu_1(\text{SO}_4)$) band at 983 cm⁻¹ that is Raman fingerprint of epsomite [e.g., 14, 15]. In Fig. 1, the same Raman peak at 983 cm⁻¹ is also visible when the solid MgSO₄·7H₂O was placed beyond a 5-cm thick layer of shaved ice. The intensity of the Raman spectrum in the shaved ice is lower because of attenuation of laser beam caused by scattering by the ice particles. The OH stretching Raman modes of epsomite appear at 3303, 3425 cm⁻¹ [14], and is largely masked by the strong OH stretching band of H₂O-ice.

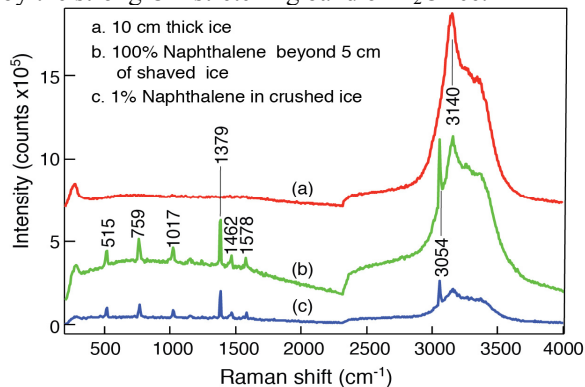


Figure 2. Raman spectra of naphthalene (1 wt %) in crushed ice, beyond 5 cm thick layer of shaved ice, and of solid water ice at 120 m. Experimental conditions were the same as in Fig. 1.

Figure 2 shows the remote Raman spectra of naphthalene (1 wt%) in the crushed H₂O-ice, beyond a 5 cm layer of shaved H₂O-ice, and 10 cm thick solid H₂O-ice. The strongest Raman fingerprint line of naphtha-

lene at 1379 cm⁻¹, and the aromatic C-H stretching mode at 3054 cm⁻¹ are clearly detected along with other strong A_{1g} modes of naphthalene molecules [e.g., 16] both in the spectra of 1 wt% naphthalene, and naphthalene buried at the depth of 5 cm in shaved H₂O-ice. Similar Raman spectra were measured from the samples of anthracene and dry ice buried within 5 cm depth of shaved ice. The strong Raman fingerprint line of anthracene at 1403 cm⁻¹, and the C-H stretching mode at 3053 cm⁻¹ [e.g., 20], and the Fermi-resonance doublet of dry-ice at 1278 and 1385 cm⁻¹ [17] were clearly detected. These observations indicate that a remote Raman instrument will be able to measure and identify various salts, organic and CO₂-ice at the surface and subsurface of Europa to a depth of a few centimeters. As the organics on the surface of Europa are most likely destroyed by the presence of strong radiation, the possibility of detecting organics in the subsurface of Europa makes remote Raman techniques on board a lander or rover an excellent instrument. Based on these results, we have estimated that with a large 1-m telescope and 355 nm pulsed laser operating at 0.5 J/pulse it will be possible to develop an orbital remote Raman instrument for mapping Europa's surface and subsurface down to 5 cm from a 10-km orbit during day-time and nighttime [e.g., 18] for future Europa missions.

Acknowledgments: This work was supported in part by the MIDP grant #NNX08AR10G.

References:

- [1] Khurana, K.K., et al (1998) *Nature* **395**, 777–780.
- [2] Kivelson, M.G., et al. (2000) *Science* **289**, 1340–1343.
- [3] Chyba, C.F. and C.B. Phillips (2001), *Proc. Nat. Acad. Sci.* **98**, 801-804.
- [4] Chyba, C.F. and C.B. Phillips (2002) *Origins Life Evol. Biosph.*, **32**, 47-68..
- [5] McCord, T.B., et al. (2001) **106**, 3311–3320.
- [6] Carlson, R.W., et al. (2009) in *Europa*, pp. 283-327, Univ. of Arizona Press.
- [7] Dalton, J.B., III, et al. (2007) *Geophys. Res Lett.*, **34**, L21205, 4 pp.
- [8] Dalton et al. (2013) *Planetary Space Sci.* **77**, 45–63.
- [9] Europa Study Team (2012) *Europa 2012 Study Report*, JPL D-71990, JPL, Pasadena, CA.
- [10] Pappalardo, R.T et al. (2013) *Astrobiology* **13**, 740-773.
- [11] Sharma, S.K., et al. (2006) *Appl. Spectrosc.* **60**, 871-876.
- [12] Misra, A.K., et al. (2012) *Appl. Spectrosc.* **66**, 1279-1285.
- [13] Abedin, M.N, et al. (2013) *Appl. Optics*, **52**, 3124-3126.
- [14] Wang, A., et al. (2006) *Geochim. Cosmochim. Acta*, **70**, 6118-6135.
- [15] Misra A.K., et al. (2007) *Proc. SPIE*, **6681**, 66810C/1-13.
- [16] Chen-Hanson, T. (1969) *J. Chem. Soc. (Taipei, Tiwan)* **16**, 123-136.
- [17] Sharma, S. K., et al. (2004) *LPSC 35*, #1929.
- [18] Angel, S.M. et al. (2012) *Appl. Spectrosc.*, **66**, 137–150.